Use of a remotely piloted aircraft system for hazard assessment in a rocky mining area (Lucca, Italy)

Riccardo Salvini[1], Giovanni Mastrorocco[1], Giuseppe Esposito[1], Silvia Di Bartolo[1], John Coggan[2], Claudio Vanneschi[2]

[1]Department of Environment, Earth and Physical Sciences and Centre of GeoTechnologies, University of Siena, Via Vetri Vecchi 34, 52027 San Giovanni Valdarno, AR, Italy
[2]University of Exeter, Camborne School of Mines (CSM), College of Engineering, Mathematics and Physical Sciences (CEMPS), Penryn, Cornwall TR10 9EZ, UK

Correspondence to: Riccardo Salvini (riccardo.salvini@unisi.it)

Abstract. The use of remote sensing techniques is now common practice in different working environments, including engineering geology. Moreover, in recent years the development of structure from motion (SfM) methods, together with rapid technological improvement, has allowed the widespread use of cost effective remotely piloted aircraft systems (RPAS) for acquiring detailed and accurate geometrical information even in evolving environments, such as mining contexts. Indeed, the acquisition of remotely sensed data from hazardous areas provides accurate 3D models and high resolution orthophotos minimizing the risk for operators. The quality and quantity of the data obtainable from RPAS surveys can then be used for inspection of mining areas, audit of mining design, rock mass characterizations, stability analysis investigations and monitoring activities. Despite the widespread use of RPAS, its potential and limitations have still to be fully understood.

In this paper a case study is shown where a RPAS was used for the engineering geological investigation of a closed marble mine area in Italy: direct ground based techniques ~~couldn't~~ could not be applied for safety reasons. In view of re-activation of the mining operations, high resolution images taken from different positions and heights were acquired and processed by using SfM techniques, for obtaining an accurate and detailed three-dimensional model of the area. The geometrical and radiometrical information was subsequently used for a deterministic rock mass characterization that led to the identification of two large marble blocks that pose a potential significant hazard issue for the future workforce. A preliminary stability analysis, with focus on investigating the contribution of potential rock bridges, was then performed in order to demonstrate the potential use of RPAS information in engineering geological contexts for geo-hazard identification, awareness and reduction.

1 Introduction

In open-pit or quarry areas, personnel and equipment involved in mining operations can be exposed to different types of slope instability processes. Rock collapses can be due to a series of predisposing and triggering factors, mostly depending on relationships between localized geological conditions and mining activities. According to Zajc et al. (2014), for example,

hazardous situations may occur when unfavourable sedimentological characteristics and geological discontinuities (e.g. joints, faults) of rock masses are made even more critical by ~~stone~~ extraction of the resource or ore material~~hazardous situations may occur when sedimentological characteristics and geological structures (e.g. joints, faults, bedding planes) of rock masses are altered by exploitation~~. In addition,~~At the same time,~~ Zheng et al. (2015) highlight~~underlain~~ the crucial role played by morphological features, such as~~like~~ sharp cuts and steep slopes, for potential~~the~~ triggering of rockfalls in mining areas. As widely demonstrated in the literature, the understanding of geometric relationships between geological discontinuities and slope morphology is essential to evaluate the potential occurrence of rock failures, since orientation of joint sets may influence both ~~the~~ size and failure mechanisms of rock blocks prone to collapse (e.g. Stead and Wolter, 2015). Generally, discontinuity characterization is carried out in the field by traditional engineering geological surveys (Priest, 1993). M~~; m~~easurements may be subjected to different source of errors which can result in either under- or over-estimation of the discontinuity geometrical properties (Tuckey and Stead, 2016). In order to avoid this deficiency Sturzenegger and Stead (2009) suggest~~ed to~~ coupling~~e~~ traditional field measurements with remote sensing techniques. Indeed, techniques such as terrestrial laser scanning (TLS) and digital terrestrial photogrammetry (DTP) for rock mass characterization are increasingly being used, especially in open pit mines where rock slopes subjected to excavation are analyzed (e.g. Kovanič and Blišťan, 2014; Salvini et al., 2015; Tuckey and Stead, 2016). TLS and ~~DP~~DTP allow accurate representation of rock~~y~~ outcrops by means of 3D point clouds or interpolated models. A limitation of ground-based remote sensing is related to the survey of complex topography from sub-optimal camera or scanner positions, resulting in occlusion zones ~~However, it is worth noting that ground-based acquisition of high resolution topographic data of complex morphologies may be very difficult to acquire because of occlusions and inaccessible zones~~ (Passalacqua et al., 2015). A solution to this problem is provided through~~by the~~ use of remotely piloted aircraft systems (RPAS), that can be used as a platform to acquire light detection and ranging (LiDAR) or photogrammetric data. ~~According to Chen et al. (2015)~~ T~~t~~here are ~~only few~~several photogrammetric studies using RPAS for the geomorphic feature characterization or mapping of the surface extent in open-pit mines~~published references related to RPAS applications in open-pit mining. The majority of photogrammetric studies deal with geomorphic feature characterization or mapping of the surface mine extent~~ (Lamb, 2000; Chen et al., 2015; Shahbazi et al., 2015; Tong et al., 2015; Esposito et al., 2017). Few studies ~~works~~ are associated with~~of them concern~~ the use of RPAS for discontinuity characterization of rock slopes affected by mining activity. Salvini et al. (2016), for example, used ~~an~~ RPAS to map discontinuities in a marble quarry and to subsequently build 3D discrete fracture network models. McLeod et al. (2013) explored the feasibility of using RPAS-acquired video images to derive 3D point clouds and to measure fracture orientations.

Digital images obtained~~acquired~~ from RPAS are commonly processed with the structure from motion (SfM) technique (Spetsakis and Aloimonos, 1991; Fonstad et al. 2013; Colomina and Molina, 2014; Westoby et al., 2012). SfM is based on sophisticated algorithms of image matching that use pseudo-random redundant images acquired from multiple viewpoints to reconstruct the three-dimensional geometry of an object or surface. In order to analyze rock outcrops, the use of RPAS multicopter~~s~~ results are particularly suitable because ~~they~~ it allow~~s~~ different geometric configurations for ~~the~~ image

Formattato: Non Evidenziato

acquisition (i.e. zenithal, frontal, oblique). Multiple images obtained from different angles help ~~both~~ the image alignment procedure and limit non-linear deformations. Moreover, the relatively short distance to which multicopters can operate from rock faces allows acquisition of high resolution images that can be used for producing high quality topographic products and subsequent interrogation.

~~However, i~~In RPAS-SfM applications particular care is needed when geo-referencing the 3D model. As stated by Passalacqua et al. (2015), sensors such as cameras or lasers fixed to RPAS typically do not have onboard navigation systems with ~~a~~ sufficient accuracy for geodetic positioning. In fact, the global navigation satellite system (GNSS) and inertial measurement unit (IMU) devices typically mounted on RPAS are used for navigation and flight stabilization purposes and allow only a rough estimation of airborne camera~~s~~ exterior orientation (Gonçalves and Henriques, 2015). In order to obtain ~~obtain~~ accurate and georeferenced ~~the~~ 3D models, the use of ground control points (GCPs) surveyed with geodetic GNSS receivers and a total station (TS) is generally employed (Francioni et al. 2015). Nevertheless, the final accuracy is dependent not only ~~from~~ on the GCP-related accuracy, density and distribution within the surveyed area, but also ~~from~~ on image quality and percentage of overlapping between single frames. Therefore, careful planning of an RPAS photogrammetric survey plays a crucial role in providing accurate results necessary for subsequent analysis, such as determination of discontinuity measurements.

In this study, two RPAS-based photogrammetric surveys were carried out within an open-pit mine of the Apuan Alps marble district, Italy. These surveys aimed to obtain detailed topographic information of the area. The 3D data was then used to perform a preliminary rockfall hazard ~~evaluation~~assessment, requested in view of a potential restart of the mining operations interrupted some years ago. Indeed, the safety of the workforce represents a critical aspect for the exploitation of the marble quarries of the Apuan Alps. ~~In the last decades, many deadly rock failures involving personnel employed in the mining activity have occurred. The last accident occurred on April 14, 2016 (Petley, 2016). In this case, two workers were killed and another injured by a large rockfall involving around 2000 tons of marble, during the excavation of a fractured rock wall.~~ The geo-structural conditions of the marble predispose the rock masses to different types of failures with different magnitudes. Slope stability analys~~e~~is are therefore essential to improve safety conditions for personnel employed in the mines. However, a complete analysis of all the slopes characterizing an open-pit mine is often problematic, given their spatial extension and limitations of numerical models. For this reason both geological and geomorphological information of the whole mining area are essential to detect and evaluate the most hazardous situations. RPAS-derived data were therefore integrated with those acquired in the field from a traditional engineering geological survey. The combined use of these data~~information~~ allowed preliminary 3D analysis and evaluation of the stability conditions of a large rock~~y~~ block that was identified as posinge~~d~~ a risk to the mining area. Nevertheless, there are controlling factors that can have a great influence on the stability condition of a block or slope that cannot be fully determined, such as ~~the case of~~ discontinuity persistence. The presence of intact rock bridges, that represent~~s~~ intervals of intact rock between adjacent discontinuities (ISRM, 1978), can significantly increase the stability of a rock slope, since the cohesion of the intact rock is generally of at least two orders of magnitude greater than the

shear strength of a discontinuity (Park, 2005). In general, joint persistence (K) is defined as the fraction area that is actually discontinuous (Einstein et al., 1983), and can be calculated with the following Eq. (1):

$$K = \lim_{A_D \to \infty} \frac{\sum_i a_{Di}}{A_D} \quad (1)$$

where D is a region of the plane with area A_D and a_{Di} is the area of the joint in D.

The limit of the application of this method is that the discontinuity area is practically impossible to measure deterministically in the field, for this reason persistence is commonly measured as trace length on rock outcrops. Jennings (1970) proposed the following Eq. (2) for persistence calculation starting from trace length values on rock exposure:

$$K = \frac{\sum JL}{\sum JL + \sum RBR} \quad (2)$$

where JL is the total length of the joints segment and RBR is the total length of rock bridges.

Mathematically, it is possible to consider the presence of rock bridges in terms of effective cohesion along the shear surface (Eberhardt et al., 2004) by using the following Eq. (3):

$$c_i = c\frac{A_g}{A} \quad (3)$$

where c is the intact rock cohesion, A_g the total area of intact rock bridges along the shear surface, and A is the total area of the shear surface.

Importantly~~Anyhow~~, as recently reported by Tuckey and Stead (2016), in spite of the importance of intact rock bridges in slope stability ~~is a well known topic qualitatively understood for decades~~, there are still no standard accepted methods for estimating the extent of rock bridges~~e contents~~ and incorporating rock bridges into slope stability analysis.

Formattato: Non Evidenziato

2 Geographical and geological setting

The study area is located in the Apuan Alps marble district, in the province of Lucca (Tuscany, Italy ~~-),~~ Fig. 1). The open pit or quarry, named "Piastrone", is characterized by a V shape, with two principal slope directions oriented 50/90 and 323/90 (dip direction/dip). The bottom of the pit is located at 1,180 meters above sea level (m.a.s.l.) and the top of the excavated rock face is at 1,300 m.a.s.l.~~The bottom of the pit is located at 1,180 meters a.s.l., but the excavated rock faces can reach and overcome 1,300 meters a.s.l.~~ The rock mass is characterized by different sets of discontinuities with persistence values that can vary from a few meters up to decameters.

From a geological point of view (Fig. 2) the Piastrone open pit is located in the Apuan Alps metamorphic complex, precisely in the Mt. Altissimo Syncline (AS), belonging to the Apuane Unit (Meccheri et al., 2007)~~, Fig. 2~~. According to classical interpretation (Carmignani and Kligfield, 1990) AS resulted from a compressive tectonic phase which originated during the Tertiary continental collision between the Sardinia-Corsica block and the Adria plate. Successively, during the Early Miocene, a new ductile to brittle-ductile deformation caused by a post-compression tectonic uplift overprinted the earlier structures and generated a widespread network of joints and faults. In the Mt. Altissimo area, the main set of ~~fragile~~ brittle

deformation strikes SW-NE to W-E with sub-vertical dip, generally with negligible displacement ~~motion~~ except for a~~rom~~ few cases where offsets of some ten meters have been observed (Meccheri et al., 2007).

AS involves the oldest ~~terms~~ lithologies of the Apuane unit sequence, ~~with~~ including pre-Alpine basement rocks, Grezzoni dolostones, megalodont-bearing marbles with metabreccias and chloritoid-rich phyllites, local lenses of dolomitic marblems and Marbles sensu stricto of lower Liassic age (Meccheri et al., 2005). Due to the compressive tectonic phase, a penetrative S1 foliation is also present in all the lithotypes (except for~~om~~ dolostones).

3 Methods

3.1 Geomatic survey

In order to assess and localize the slope stability hazard in the rocky mining area, two RPAS surveys were carried out with direction of photo~~s~~ acquisition in zenithal modality (~~on the~~ perpendicular to~~above~~ the open pit floor) and in frontal modality (~~on the~~ perpendicular to the rock faces). ~~two RPAS surveys were carried out in zenithal modality and in a parallel direction to the rock faces (frontal).~~ The surveys were performed in December 2015 using the Aibotix™ Aibot X6 V1 multicopter, which has~~composed by~~ six electric rotors, and equipped with a Nikon™ CoolpixA digital camera (Table 1) and a GNSS/IMU system that allows recording of 3D coordinates (X0,Y0,Z0) and orientation of the camera (pitch, roll and yaw – ω ϕ κ) at every shoot or image.

The zenithal survey was preliminarily designed in the laboratory with the Aibotix™ Aiproflight planning software, and manually performed through single quasi-parallel flight lines. A total of 151 aerial images were acquired with a nominal overlap and sidelap of 80% and 60% respectively. Two flights were required~~needed~~ to cover all sectors of the mining area (Fig. 3).

An average estimated distance between pixel centers measured on the ground (i.e. ground sample~~ing~~ distance ~~(~~ - GSD) of 2.4 cm was calculated. During the flight, a global navigation satellite system (GNSS) field survey was also carried out in order to ensure the necessary spatial accuracy of the resultant~~for the exterior orientation of the~~ images. ~~, measuring a total of~~Eight ~~8~~ artificial targets, 50x50 cm large, were uniformly distributed over the study area (Fig. 4) and~~and~~ used as ground control points (GCPs) and check points.

The GNSS survey was carried out in ~~Real~~ real ~~Time~~ time ~~Kinematic~~ kinematic (RTK), using geodetic receivers. A~~In particular, a~~ reference station was set up, recording continuous signals from the GNSS satellite constellation for more than~~above~~ 3 hours. The positional information obtained~~acquired~~ by the reference station was then sent to a mobile receiver, using ~~a~~ radio modem communication. Each ground control point, GCP, was occupied for at least two minutes with a recording interval equal to 1 second. The coordinates of the points determined~~acquired with~~ using this technique were corrected by post-processing procedures using contemporary data recorded by three permanent GNSS stations (La Spezia, Pieve Fosciana and Pisa) allowing centimetric accuracy. The orthometric heights were also calculated by using Convergo, an Italian code for full coordinate~~s~~ conversion. The coordinates of the GCPs were collected in ETRF2000 and then converted

toin the Italian National Gauss Boaga system for the exterior orientation of the images and subsequent determination of the inclination and positionrestitution of slopes and orientation of discontinuitiesjoints orientation.

The frontal survey, with directions of acquisition parallel to the rock faces, was carried out manually, without the use of the Aibotix™ AiProflight planning software. Six flights were required in orderneeded to cover all sectors of the mining area, resulting in for a total of 448 overlapping images. The flights were executed inaccording to sub-parallel straight lines approximatelybout 60 meters distant from the rock face (Fig. 5), providing an average estimated GSD of 1.5 cm.

As for the zenithal flight, a series of GCPs and check points (21 targets in total - Fig. 6) were measured usingby a reflectorless total station (TS). Due to the complex morphology of the slopes and the extent of the mining area, a large number of GCPs were used to orient the photogrammetric model. Two GNSS receivers, operating in static modality, were used to obtain the geographic coordinates of two points: the origin of the survey and its zero-Azimuth direction. FAlso for this survey, GNSS data were corrected using contemporary data recorded by permanent GNSS stations and ellipsoidal heights were converted to orthometric heights.

3.2 Application of structure from motion algorithms

The software Agisoft™ PhotoScan Professional version 1.2.5 (Agisoft 2016) was used to process the images obtained fromwith the two RPAS surveys (two zenithal flights plus six frontal flights). This software is capable ofto solvinge the camera interior and exterior orientation parameters and to generate georeferenced spatial data such aslike 3D point clouds, digital surface models (DSMs) and orthophotos. All the images acquired fromin the two surveys were processed with an identical photogrammetric processing, in two distinct Agisoft™ Photoscan projects;, one for the zenithal flights and another for the frontal flights.

The first processing step consisted ofin the image alignment, through which the interior and relative orientation parameters were solved. In order to improve the whole alignment process and to obtain low re-projection error, millions of tie points were automatically extracted without setting a point limit. As result of the previous stage, all images were aligned. Following image alignment, tThe second processing step involved georeferencing of the 3D model in such a way as to solve the exterior orientation parameters by using the GCPs coordinates measured during the two GNSS-TS topographic surveys. For both surveys, a number part of the measured points wereas used as check points to verify the model accuracy. Specifically, for the zenithal survey 2 of the 8 measured target points were used as check points, while for the frontal survey (with directions of photo acquisition parallel to the rock faces), 4 points out of 21 were used as check points. Both natural and artificial targets were identified directly on the images, assigning a 3D coordinate to each of them.

Subsequently, the 'optimize' tool was utilized in order to adjust the estimated camera positions tofor removeing possible non-linear deformations, minimizing the errors due to re-projection and misalignment of the photos. Moreover, the optimization was improved by deleting all the tie points with a re-projection error greater than 1 pixel.

In a subsequent step, the zenithal and frontal dense 3D point clouds were generated with medium quality and aggressive depth filtering settings. No automatic classification of clouds was necessary: no infrastructure was present as the mine was not operational and there was no vegetation within the area of interest.

FinallyLastly, a polygonal 3D mesh model was created from the point cloud and used to create the orthophoto of the open pit area. The orthophoto has the property of been removed from image distortions removed due to camera characteristics (i.e. lens distortions), camera tilt and topographic relief displacement. Unlike an uncorrected aerial photograph with a perspective projection, an orthophoto is geometrically corrected ('orthorectified') and can be used to measure true distances since it is 'scale-corrected'. The corrected orthophoto image with a spatial resolution of 1 cm/pixel was thenfinally projected into the Italian National Gauss Boaga system.

3.3 Engineering geological investigation

In order to characterize the rock mass within the open pit mine, a relatively large number of discontinuities wereas identified directly on the dense point cloud. The orientation of the selected discontinuitiesjoints was manually calculated by creating patches that best fit the identified discontinuity planes in the point cloud and extracting their orientation using the Leica™ Cyclone 9.0 software. DThe discontinuity sets were then identifiedrecognized using stereographic representation (Schmidt equal-area method, lower hemisphere).

According to Mastrorocco et al. (2017), a manual deterministic fracture mapping was also adopted because it increases the level of control of the process, that is essential where the morphology of the quarry slope surfaces is largely artificial (smooth cut surfaces). The collected point cloud-derived data were then compared with those manually measured by traditional engineering geological surveys. On the basis of engineering geological data, the geological strength index (GSI - Hoek and Brown, 19971994) and the rock mass rating (RMR - Bieniawski, 1989) characterization were also applied, and a kinematic stability analysis was carried out using the Markland test (Markland, 1972). The latter testing was undertaken in order to identify potential kinematic failure mechanisms that characterize the slopes. The tests for planar sliding, wedge sliding, and direct toppling were conducted for both principal slope directions (Eastern slope - dip direction/dip 50/90; Western slope - dip direction/dip 323/90).

Despite the importance of performing kinematic analysis to discover the possible block instability, one of the principal limitations of this stereographic method is the inability to locate the block source areas on the slope being analyzed. For this reason, the most critical blocks have been identified directly on the point cloud. The points representing the geometry of every single block were meshed in Leica™ Cyclone 9.0 and their volume estimated usingin respect of reference planes corresponding to the discontinuities that demarcate or shape the respective blocks.

The collected orientation data were finally used for preliminary stability analyses using Rocscience™ Swedge software. Swedge is a 3D software for evaluation ofng the stability of surface wedges in rock slopes. It considers the intersection of discontinuities and allows the calculation of safety factors of the formed blocks. The software is based on classical limit equilibrium methods that usually have some limitations, such as lack of consideration of in-situ stress, strains and intact

material failure (Stead et al., 2006). Nevertheless, Swedge does allow ~~the~~ consideration of external forces, by applying a force (vector with given orientation and intensity) to the formed blocks. From this, preliminary analysis of the impact of water content or other forces can also be performed. The software can also be used to assess the stability of wedges formed by a basal plane.

4 Results

4.1 Photogrammetric modelling

The image alignment process, described in section~~paragraph~~ 3.2, resulted in a re-projection error related to the manual placement of GCPs on the images of 0.41 pixel for the zenithal survey and 0.48 pixel for the frontal survey. The final ~~Root~~ root ~~Mean~~ mean ~~Square~~ square ~~Error~~ error (RMSE) for the zenithal flights exterior orientation was equal to 0.042 meters; RMSE for the frontal flights exterior orientation was equal to 0.043 meters (Table 2).

The final 3D frontal and zenithal point clouds contain~~are constituted by~~ more than 18,000,000 and almost 13,000,000 ~~of~~ points respectively, with a mean point spacing varying from 1 to 4 cm.

4.2 Rock~~y~~ slope engineering geological characterization

The orientation of 154 discontinuity planes manually selected on the point cloud was calculated through stereographic projection. The final stereonet allowed ~~to identify~~identification of four discontinuity sets, whose properties listed in table 3 were obtained from traditional engineering geological survey carried out in accessible areas of the mine~~are listed in table 3~~. ~~Figure 7 shows a comparison between the latter (b) and the stereonet obtained through traditional manual engineering geological survey (a), highlighting a good level of congruence that confirms the quality of the taken approach~~By comparing the discontinuity planes obtained through traditional manual engineering geological survey (a in Fig. 7) and that identified on the point cloud (b in Fig. 7) ~~.~~a good level of congruence has been highlighted, confirming the quality of the approach taken ~~approach~~.

Based on the discontinuity characteristics derived from ~~the~~ RPAS and traditional engineering geological surveys, the basic RMR (RMRb) and GSI index were calculated. The RMRb was found to be 67 (table 4), while the GSI was estimated to be between 60 and 65 using the modified chart proposed by Hoek et al. (2013)~~to be between 60 and 65~~. In addition, application of Hoek et al. (2013) equation for GSI quantification (GSI=1.5 $JCond_{89}$ + RQD/2) confirmed the results of the qualitative chart interpretation with a value of 65~~4.5.~~,

B~~Therefore, both classifications indicating~~ indicated ~~in both cases~~ a rock mass of 'good' quality. These results agree with the authors' field observations and what is described in the actual quarry excavation plan (Lorenzoni, 2012). In view of the rock competency, potential instability is not related to the strength properties~~general weaknesses~~ of the rock mass, but the intersection of discontinuity planes can locally form ~~isolate~~ rock~~y~~ blocks with the potential for sliding or toppling. For this reason, a kinematic stability analysis was performed. A discontinuity friction angle of 35° was used in the analysis: this

Formattato: Pedice

agrees with data from previous studies carried out by the quarry's advisors (Lorenzoni, 2012; Dumas, 1999), by the Geomechanical laboratory of the Centre of GeoTechnologies of Siena University, and literature (Chang et al., 1996~~;~~ Perazzelli et al., 2009~~;~~ Mastrorocco, 2013) ~~and~~. Table ~~4~~ 5 shows the potential failures identified through kinematic stability analysis (examples are shown in Fig. 8) for both principal slope orientations. Three different possible kinematic modes~~sms~~ were identified, with K2b and K4 systems ~~that~~ have~~ing~~ the most influence on ~~the~~ potential instability. T~~In regard to this, the~~ majority of the potential failures identified~~are~~ related to planar sliding or wedge sliding, in agreement with field and SfM~~-~~based observations.

~~Results~~ Therefore~~,~~ results highlight the potential for blocks to form ~~of variable shape and size, varying from about a cubic meter to a few hundred cubic meters,~~ that may be subject to gravity induced instability but, as previously stated, traditional kinematic analyses do not identify the ~~n't allow~~ location~~lization~~ of these ~~potential~~ unstable blocks. Therefore, further analysis of the high resolution images and the dense point cloud was performed~~ere analyzed~~ in order to locate possible block source areas. More than 20 blocks were deterministically characterized in terms of size, shape and barycentric coordinates, varying from about a cubic meter to a few hundred cubic meters. In addition~~particular~~, t~~T~~he analysis~~dopted approach also~~ identified two large blocks (Fig. 9), a few thousand cubic meters in size, with potential for sliding. These are ~~shown in Fig. 9, and are~~ formed by the intersection of two different faults and a discontinuity basal plane with 5 cm aperture, no infill, smooth surface and high persistence. The basal plane appears not to~~doesn't~~ correspond with~~to~~ any of the identified discontinuity sets, but ~~it~~ is probably connected to planes of weakness of the marble in correspondence with a particular orientation of minerals crystallographic axes. The ~~Differently the two faults,~~ lateral and rear faults, however~~back~~, may be ~~respectively~~ associated with~~to systems~~ the K3a and K3b systems respectively. The rear~~In particular the back~~ fault may also be associated with the~~can be contextualized from a geological point of view in a~~ East-West fault system that characterizes the geology of this area of the Apuan Alps complex (Fig. 2).

The geometric characteristic~~s~~ of the two blocks, including orientation of the intersecting discontinuities and volume of the meshed block, were obtained using Leica™ Cyclone 9.0 and are shown in table ~~5~~6.

The first block, Block A, is of particular interest because it daylights in the face and prevents Block B from sliding (similar to an active-passive wedge; Prandtl's prism transition zone - Kvapil and Clews, 1979). A main road access to the quarry is located at the base of this slope, increasing the potential risk for the area.

~~The geometric characteristic of the two blocks, including orientation of the intersecting discontinuities and volume of the meshed block, were obtained using Leica™ Cyclone 9.0 and are shown in table 5.~~

Due to the particular geometrical configuration, Block A can be described as the key block as it daylights the rock face. In the actual setting Block B does not hold the potential for sliding as it does not daylight in the slope face, but it could play a significant role in terms of additional weight force. Nevertheless, the following preliminary stability analysis is focused on Block A. Further investigation would require an analysis of the effect of Block B on the potential for instability as this provides the 'active' component of the active-passive wedge.

Formattato: Evidenziato

Formattato: Colore carattere: Automatico

4.3 Preliminary slope stability analysis

The geometry of Block A was deterministically re-created in Swedge using the geometrical information obtained from the point cloud provided in table ~~5~~6, with a slope direction of 30 degrees. Initially the discontinuities were assumed to be fully persistent. This is a common approach in engineering geology, since reliable values of persistence are almost impossible to obtain from field mapping and most rock slope stability analysis assume that the 100 % persistent joint exists on failure surface (Park, 2005). Moreover, in this case two discontinuities (lateral and rear or back surfaces) correspond to geological faults and can be therefore considered fully persistent. However, the basal plane is a joint and the possible presence of rock bridges should be carefully considered. ~~In general, joint persistence (K) is defined as the fraction area that is actually discontinuous (Einstein et al., 1983), and can be calculated with the following Eq. (1):~~

~~$$K = \lim_{A_D \to \infty} \frac{\Sigma_1 a_{Di}}{A_D} \quad (1)$$~~

~~where D is a region of the plane with area A_D and a_{Di} is the area of the joint in D.~~

~~The limit of the application of this method is that the discontinuity area is practically impossible to measure deterministically be determined in the field. For this reason, Einstein et al. (1983) proposed a rough quantification of persistence value by measuring trace length on a rock exposure. Jennings (1970) proposed the following Eq. (2) for persistence calculation starting from trace length values on rock exposure:~~

~~$$K = \frac{\Sigma JL}{\Sigma JL + \Sigma RBR} \quad (2)$$~~

~~where JL is the total length of the joints segment and RBR is the total length of rock bridges.~~

In this case the basal plane did not show the presence of segments of intact rock along its trace on the rock exposure, consequently application of Eq. (2) confirms a 100 % persistence of the basal plane, that was used in the first analysis.

The adopted limit equilibrium solution for the slope stability analysis was based on the Mohr-Coulomb shear strength model with a friction angle of 35° and a unit weight of 0.026 MN/m^3 (Ertag, 1980~~;~~ Dumas, 1999). It should be noted that the western lateral surface observable in the model was also necessary to re-create the block geometry in the software. It was assigned 0° friction angle so as not to induce a resisting force in the simulation. Water forces were also initially ignored within the preliminary analysis (Fig. 10). ~~The result of the analysis is shown in Fig. 10.~~

The result highlights a possible condition of instability for Block A which does not match with field observations, since the block under study has remained stable in this position for tens of years. In order to investigate the effect of uncertainty or variability of the input parameters, a sensitivity analysis was performed. In a sensitivity analysis (Fig. 11) specific parameters are varied across a range of values and the effect on the Factor of S~~s~~afety is observed ~~factor~~. This helps to identify the parameters that have the most effect on block stability. Since the geometrical inputs are well defined through the accurate 3D model, the subsequent analysis focused on waviness angle (it accounts for the undulations of the joint surface, observed over distances on the order of 1 m to 10 m; Miller, 1988), cohesion and friction angle of the basal plane and water pressure. These are also the parameters with the higher input uncertainty. ~~Figure 11 shows the result of the sensitivity analysis performed on the cited values.~~

Formattato: Evidenziato
Formattato: Evidenziato
Formattato: Evidenziato
Formattato: Evidenziato
Formattato: Evidenziato
Formattato: Evidenziato
Formattato: Evidenziato
Formattato: Evidenziato
Formattato: Evidenziato
Formattato: Evidenziato
Formattato: Evidenziato
Formattato: Evidenziato
Formattato: Evidenziato
Formattato: Evidenziato

As observed, the cohesion is clearly the parameter that has the most effect on block stability. For this reason, the effect of this parameter was investigated in more detail in the following analyses. ~~In practice, in rock slopes, the cohesion of intact rock bridges between discontinuous joints increases the shear strength of the surface. This can be one to two orders of magnitude greater than the shear strength available on the discontinuity (Park, 2005). Mathematically, it is possible to consider the presence of rock bridges in terms of effective cohesion along the shear surface (Eberhardt et al., 2004) by using the following Eq. (3):~~

~~$c_r = c\frac{A_B}{A}$ (3)~~

~~where c is the intact rock cohesion, A_B the total area of intact rock bridges along the shear surface, and A is the total area of the shear surface.~~ Application of Eq. (3) makes it possible to determine an effective cohesion dependent on the continuity of jointing. From this the contribution of eventual rock bridges on the block stability can be investigated starting from intact rock cohesion material value, that has been determined to be approximately 16 MPa (Lorenzoni, 2012; Dumas, 1999; data from Geomechanical laboratory of the Centre of GeoTechnologies of Siena University). Table ~~6~~ 7 shows the results in terms of factor of safety obtained from a parametric ~~in~~stability analysis performed with increased values of effective cohesion, corresponding to 0, 0.5, 1, 2, 5, and 10 % of rock bridges on the basal plane (total area of 510 m^2), and a 20 % of water filled fissures (considered reliable after field observation and high resolution images analysis).

Formattato: Evidenziato
Formattato: Evidenziato
Formattato: Evidenziato
Formattato: Evidenziato
Formattato: Giustificato
Formattato: Evidenziato
Formattato: Evidenziato
Formattato: Evidenziato
Formattato: Evidenziato

5 Discussion

The RPAS approach adopted in this case study, based on the combined use of high-resolution images from different perspective and accurate GNSS/TS topographic surveys, overcame data acquisition difficulties related to high steep quarry walls and provided high-resolution orthophotos of the site (1 cm pixel size). The application of RPAS instrumentation was extremely successful for ~~the~~ reconstruction of the complex morphology of the mine site where ground ~~–~~based techniques (e.g. terrestrial laser scanning, terrestrial photogrammetry) have limitations due to potential "shadow" effects and several inaccessible set-up zones due to safety reasons. GCPs measured using a TS and GNSS receivers permitted a high level of accuracy in the images external orientation, which is particularly important for subsequent discontinuity measurements. On the other hand, possible limitations in the use of RPAS system can be related to the need for a pilot license and user experience on topographic survey and imagery processing. Indeed, the accuracy of the final 3D model can be greatly affected by the quality of data collected (photos and GCPs), hardware and software capability and user expertise.

Although several authors have demonstrated the reliability of automatic and semi-automatic processing of imagery and 3D point clouds for fracture mapping (Mah et al. 2011; Vöge et al. 2013; Assali et al. 2014; Vasuki et al. 2014), a complete manual approach was adopted in this analysis to guarantee consistency and quality in the interpretation of discontinuities. Note that in most cases the flat and regular morphology of quarry walls only allow photointerpretation of discontinuity traces. Final visual inspection and validation of outputs is always required, even when using codes for the semi-automatic extraction of joints (Salvini et al., 2016). Therefore, the orientation of several discontinuity planes was calculated using

Leica™ Cyclone 9.0 on the point cloud, once its high positional accuracy level was demonstrated. This allowed for a more complete characterization of the rock mass than ~~the one~~ that ~~can be~~ which could be obtained through traditional engineering geological survey, due to limited safe access to the slopes within the site. This was particularly important also because discontinuity~~ies~~ characteristics can vary at different heights of the rock mass due to stress relaxation induced by excavation activity. In this context, the possibility to inspect the mining area from different angles in high definition, allowed identification of critical areas to be analyzed in detail for safety purposes. Moreover, the possibility to use the point cloud for obtaining geometrical characteristics of blocks represented a major advantage, because it allowed the exact geometrical reconstruction of a 3D model to be used in specific software for slope ~~in~~stability analysis.

In this work a potential significant risk was identified for the future workforce due to the presence of two major blocks with potential for sliding. In fact, with conservative assumptions the preliminary limit equilibrium analysis showed that the key Block A, in its present shape, is potentially unstable. This is mainly due to the fact that the basal plane dips out of the slope and daylights on the face, with a dip angle higher than the friction angle of the surface. Moreover, the block is separated from the rock mass by a major fault, that can be simulated in the Swedge analysis as a tension crack. The fault can be clearly identified from the orthophoto obtained from the application of SfM method. ~~Figure 12 shows an~~ An apparent motion has been identified on the back fault (Fig. 12). ~~From a geological point of view the fault can be contextualized in a East-West system that characterize this area of the Apuan Alps complex (, as observable in Fig. 2).~~ The presence of cataclasite with variable thickness can also be an indication of potential for ~~interpreted as another sign of~~ movement on the fault surface~~that released the block from the rock mass, similarly to the fault that acts as lateral release surfaces~~.

In this stability analysis~~context~~ the major uncertainty is on the basal plane (Fig. 12). Despite the presence of a continuous trace line on the rock exposure, its full persistence in the rock mass is not clear. In general, the presence of rock bridges plays an important role in stabilizing the removable rock blocks. In particular, a rock block cannot fall or slide from a slope until the rock bridges have failed. The rock bridge failure involves the collapse or failure of the intact rock, which can be an order of magnitude stronger than the rock mass (~~Kemeny,~~Kemeny and Donovan, 2005). From the sensitivity analysis undertaken, cohesion of the basal plane was the parameter that had~~s~~ the most significant influence on the block factor of safety. This suggests that it may not be completely persistent in this case, since the block has remained stable over time. In this regard, the parametric analysis carried out increasing the cohesion values shows how a small rock bridge, corresponding to 1% of the basal plane surface (5.1 m^2 of intact rock) is sufficient for guaranteeing the stability of the block. This is mainly due to the fact that, despite the basal plane dipping~~s~~ more than the friction angle of the surface, its inclination is not sufficient to avoid the generation of a high normal force that increases the shear strength of the discontinuity. Therefore, even a small area of intact rock increases the resisting force that leads to a condition of stability. In this case, 5.1 m^2 of rock bridge corresponds theoretically to a resisting force of 81.7 MN. Similar values of rock bridge~~s~~ percentage have also been found in different case studies, where back-analysis revealed low values of estimated rock bridge content at the moment of failure, in the order o~~f~~f 0 to 5 % (Frayssines and Hantz, 2006; Grøneng et al., 2009; Sturzenegger and Stead, 2012; Matasci et al., 2014;

Formattato: Non Evidenziato

Formattato: Non Evidenziato

Formattato: Non Evidenziato

Tuckey and Stead, 2016). Therefore, a small amount of rock bridge may be sufficient for guaranteeing stability of a rock slope.

In reality, based on field observation and authors' experience in similar contexts, higher percentage of rock bridges may exist, that could lead to increased safety. Nevertheless, Hudson and Priest (1983) identified two kinds of persistence relative to impersistent or intermittent joints that should be considered. Differently from impersistent joints, intermittent discontinuities require a network of joint segments and intact regions on the same plane. However, as described by Mauldon (1994), the formation of intermittent joints is geologically unlikely, unless weakness planes exist within the rock mass. From this it follows that the cohesion of rock bridges in intermittent joints could be much lower than that of the intact rock. This could be the case of Block A, and the presence of a series of discontinuities with similar dip and dip direction to the basal plane~~, observable in Fig. 13,~~ seems to confirm the hypothesis of a preferential plane of weakness due to the geomechanical characteristics of the marble material in that portion of the mining area (Fig. 13).

Moreover, the progressive degradation with time of rock bridge~~s~~ elements could cause a progressive failure mechanism that has the potential to lead to a final rockfall event. This is particularly important in small engineered slopes such as the present one, where the rock mass may be continuously disturbed by excavation activity driving the slope to instability. Such mechanisms of progressive brittle fracturing of rock bridges are not considered in limit equilibrium approaches, and it is a known key limitation (Tuckey and Stead, 2016). The result is that when using the Mohr-Coulomb shear strength criterion, inclusion of a small content of rock bridges adds significant apparent cohesion to the failure surface (Elmo et al., 2011; Tuckey and Stead, 2016).

The aspects discussed in this section lead to the conclusion that a potentially hazardous situation should not be underestimated. Therefore, in case of re-opening of mining activities an in-depth engineering geological analysis, together with the installation of a monitoring system for observing the behavior of the rock mass over time should be considered.

6 Conclusion

The case study highlights the powerful use of RPAS technology for rock slope characterization and acquisition of accurate 3D data for subsequent ~~in~~stability analysis. Specifically, an Aibotix™ Aibot X6 six-rotor multicopter was employed to obtain high resolution topographic data of a blocky rock mass located within a quarry prone to discontinuity-controlled instability mechanisms. A detailed 3D model of the area allowed accurate identification and geometrical measurement of the geological discontinuities that isolate significant volumes of rock~~s~~. The stability analysis performed with Rocscience™ Swedge software showed that rock bridges can have a significant influence on stability conditions. The analysis highlighted the need for further detailed analysis and installation of suitable monitoring systems for future quarry operations.

These results confirm the reliability of the employed technologies to provide data for preliminary evaluation of the hazard affecting the study area. The RPAS allowed acquisition of high resolution topographic data in an area characterized by a complex morphology where ground-based techniques would have significant limitations (e.g. terrestrial laser scanning,

Formattato: Non Evidenziato

Formattato: Non Evidenziato

photogrammetry). It is worth noting that in mountainous environments, the use of RPAS has to be evaluated according to the local atmospheric and topographic conditions. The high temporal and spatial variability of the atmospheric conditions at high altitudes, as well as the presence of vegetation or steep and irregular slopes, could endanger the flight operations. This requires pilots with relevant experience and RPAS equipped with innovative systems to manage emergency conditions. Future analysis at this site will concentrate on the evaluation of the most useful countermeasures to reduce the risk conditions, by monitoring the unstable slopes and undertaking further ~~in~~stability analysis including more complex 3D discrete fracture network (DFN) evaluation to assess the effects of rock bridges and elasto-plastic numerical approaches to assess likely instability.

Acknowledgments

Part of the present study was undertaken within the framework of an agreement with USL1 of Massa and Carrara (Mining Engineering Operative Unit - Department of Prevention). The authors acknowledge M. Pellegri and D. Gullì (USL1) and V. Lorenzoni (Professional geologist) for their support of this research.

References

Agisoft: Agisoft PhotoScan User Manual Professional Edition, Version 1.2.5, 97 pp., 2016.

Assali, P., Grussenmeyer, P., Villemin, T., Pollet, N., and Viguier, F.: Surveying and modeling of rock discontinuities by terrestrial laser scanning and photogrammetry: Semi-automatic approaches for linear outcrop inspection, J. Struct. Geol., 66, 102-114, 2014.

Bieniawski, Z.T.: Engineering Rock Masses Classification, Wiley, New York, 251 p., 1989.

Chang, C.T., Monteiro, P., Nemati, K., and Shyu, K.: Behavior of Marble under compression, J. Mater. Civil Eng., 8, 157-170, 1996.

Chen, J., Li, K., Chang, K.-J., Sofia, G., and Tarolli, P.: Open-pit mining geomorphic feature characterisation, Int. J. Appl. Earth Obs., 42, 76-86, 2015.

Carmignani, L., and Kligfield, R.: Crustal extension in the Northern Apennines: the transition from compression to extension in the Alpi Apuane core complex, Tectonics, 9, 1275-1303, 1990.

Colomina, I., and Molina, P.: Unmaned Aerial Systems for Photogrammetry and Remote Sensing: A Review. ISPRS J. Photogramm., 92, 79-97, 2014.

Dumas, F.: Variante al piano di coltivazione della cava Piastrone, sita in loc. Retro Altissimo comune di Seravezza (LU), Technical report, Henraux S.p.A., Querceta, Lucca, 36 pp., 1999.

Eberhardt, E., Stead, D., and Coggan, J.S.: Numerical analysis of initiation and progressive failure in natural rock slopes-the 1991 Randa rockslide, Int. J. Rock Mech. Min., 41, 69-87, 2004.

Einstein, H.H., Veneziano, D., Beacher, G.B., and O'Reilly, K.J.: The effect of discontinuity persistence on rock slope stability, Int. J. Rock Mech. Min., 20, 227-236, 1983.

Elmo, D., Clayton, C., Rogers, S., Beddoes, R., and Greer, S.: Numerical simulations of potential rock bridge failure within a naturally fractured rock mass, Proceedings of the 2011 International Symposium on Slope Stability in Mining and Civil Engineering, Vancouver, Canada, 18-21 September 2011, pp. 13, 2011.

ERTAG: I Marmi Apuani, Regione Toscana, Firenze, pp. 175, 1980.

Esposito, G., Mastrorocco, G., Salvini, R., Oliveti, M., and Starita, P.: Application of UAV photogrammetry for the multi-temporal estimation of surface extent and volumetric excavation in the Sa Pigada Bianca open-pit mine, Sardinia, Italy, Environ. Earth Sci., 76:103, doi:10.1007/s12665-017-6409-z, 2017.

Fonstad, M. A., Dietrich, J. T., Courville, B. C., Jensen, J. L., and Carbonneau, P. E.: Topographic structure from motion: a new development in photogrammetric measurement, Earth Surf. Proc Land., 38, 421-430, 2013.

Francioni, M., Salvini, R., Stead, D., Giovannini, R., Riccucci, S., Vanneschi, C., and Gullì, D.: An integrated remote sensing-GIS approach for the analysis of an open pit in the Carrara marble district, Italy: Slope stability assessment through kinematic and numerical methods. Comput. Geotech., 67, 46-63, 2015.

Frayssines, M., and Hantz, D.: Failure mechanisms and triggering factors in calcareous cliffs of the Subalpine Ranges (French Alps), Eng. Geol., 86, 256-270, 2006.

Giglia, G., and Paiotti M.: Carta Geologica delle Alpi Apuane, M. Altissimo, Geological map, 1963.

Gonçalves, J. A., and Henriques, R.: UAV photogrammetry for topographic monitoring of coastal areas, ISPRS J. Photogramm., 104, 101-111, 2015.

Grøneng, G., Nilsen, B., and Sandven, R.: Shear strength estimation for Åknes sliding area in western Norway, Int. J. Rock Mech. Min. Sci., 46, 479-488, 2009.

Keywords: Rockslide; Sliding plane; Shear strength; Triaxial tests; Barton–Bandis empirical method

Hoek, E.: ~~and Brown, E.T.: Practical estimates of rock mass strength, Int. J. Rock Mech. Min. Sci., 34, 1165-1186, 1997~~ Strength of rock and rock masses, ISRM News J., 2, 4-16. 1994.~~.~~

Hoek, E., Carter, T.G., and Diederichs, M.S.: Quantification of the Geological Strength Index Chart, Proocedings of 47th US Rock Mechanics/Geomechanics Symposium, San Francisco, USA, 23-26 June, 2013.

Hudson, J.A., and Priest, S.D.: Discontinuity frequency in rock masses, Int. J. Rock Mech. Min., 20, 73-89, 1983.

Jennings, J.E.B.: A mathematical theory for the calculation of the stability of slopes in open cast mines, Proocedings of Symposium on the Theoretical Background to the Planning of Open Pits Mines with Special Reference to Slope Stability, Johannesburg, South Africa, 29 August - 4 September, 87-102, 1970.

International Society for Rock Mechanics (ISRM): Commission on standardization of laboratory and field test:suggested methods for the quantitative description of discontinuities in rock masses. Int. J. Rock Mech. Min. Sci. Geomech. Abstr., 15, 319-368, 1978.

Kemeny, J., and Donovan, J.: Rock mass characterization using LiDAR and automated point cloud processing, Ground Eng., 38, 26-29, 2005.

Kovanič, L., and Blišťan, P.: Quarry wall stability assessment using TLS method, Advanced Materials Research Vols., 1044-1045, 603-606, 2014.

Kvapil, R., and Clews, K.M.: An examination of the Prandtl mechanism in large-dimension slope failures, Trans. Inst. Min. Metall., Sect. A: Mining Industry, 88, A1-A5, 1979.

Lamb, A. D.: Earth observation technology applied to mining related environmental issues, Min. Tech., 109, 153-156, 2000.

Lorenzoni, V.: Progetto di coltivazione della cava "Piastrone" comune di Seravezza, provincia di Lucca, Technical report, comune di Seravezza, Lucca, 18 pp., 2012.

Mah, J., Samson, C., and McKinnon, S.: 3D laser imaging for joint orientation analysis, Int. J. Rock Mech. Min. Sci., 48, 932-941, 2011.

Formattato: Inglese (Regno Unito)

Formattato: Inglese (Regno Unito)

Formattato: Inglese (Regno Unito)

Formattato: Italiano (Italia)

Formattato: Italiano (Italia)

Formattato: Apice

Markland, J.T.: A useful technique for estimating the stability of rock slopes when the rigid wedge slide type of failure is expected: Imperial College Rock Mechanics Research Reprints, 19, 10 pp., 1972.

Mastrorocco, G.: Analisi della stabilità di una cava di marmo in sotterraneo nelle Alpi Apuane: Laser scanning terrestre, metodi convenzionali e modellazione numerica, Master of Science thesis, University of Siena, Italy, 185 pp., 2013.

Mastrorocco, G., Salvini, R., and Vanneschi, C.: Fracture mapping in challenging environment: a 3D virtual reality approach combining terrestrial LiDAR and high definition images, Bull. Eng. Geol. Env., doi:10.1007/s10064-017-1030-7, 2017.

Matasci, B., Jaboyedoff, M., Ravanel, L., and Deline, P.: Stability Assessment, Potential Collapses and Future Evolution of the West Face of the Drus (3,754 m asl, Mont Blanc Massif), in: Engineering Geology for Society and Territory vol. 2, Springer International Publishing, 791-795, 2015.

Mauldon, M.: Intersection probabilities of impersistence joints, Int. J. Rock Mech. Min., 31, 107-115, 1994.

McLeod, T., Samson, C., Labrie, M., Shehata, K., Mah, J., Lai, P., Wang, L., and Elder, J. H.: Using video acquired from an Unmanned Aerial Vehicle (uav) to measure fracture orientation in an open-pit mine, Geomatica, 67, 173-180, 2013.

Miller, S.M.: Modeling Shear Strength at Low Normal Stresses for Enhanced Rock Slope Engineering, Proceedings of 39th Highway Geology Symposium, 346-356, 1988.

Meccheri, M., Berretti, G., Conti, P., and Molli, G.: Interference structures at the southern closure of the M. Altissimo Syncline, central Alpi Apuane, Italy, Rend. Soc. Geol. It., 1, 123-124. 2005.

Meccheri, M., Bellagotti, E., Berretti, G., Conti, P., Dumas, F., Mancini, S., and Molli, G.: The Mt. Altissimo marbles (Apuan Alps, Tuscany): commercial types and structural setting, Ital. J. Geosci., 126, 22-35. 2007.

Park, H.J.: A new approach for persistence in probabilistic rock slope stability analysis, J. Geosci., 9, 287-293, 2005.

Passalacqua, P., Belmont, P., Staley, D., Simley, J., Arrowsmith, J. R., Bodee, C., Crosby, C., DeLongg, S., Glenn, N., Kelly, S., Lague, D., Sangireddy, H., Schaffrath, K., Tarboton, D., Wasklewicz, T., and Wheaton, J.: Analyzing high resolution topography for advancing the understanding of mass and energy transfer through landscapes: A review, Earth-Sci. Rev., 148, 174-193, 2015.

Perazzelli, P., Rotonda, T., and Graziani, A.: Stability analysis of an active marble quarry by DEM modelling, in: Proceedings of the International Conference on Rock Joints & Jointed Rock Masses, Tucson, Arizona, USA, 7-8 January 2009, 8 pp., 2009.

~~Petley, D.: Colonnata: a large collapse in a Carrara marble quarry in Italy, The landslide blog-AGU blogosphere, available at: http://blogs.agu.org/landslideblog/2016/04/15/colonnata-1/, last access: 4 April 2017, 2016.~~

Priest, S. D.: Discontinuity analysis for rock engineering. Chapman & Hall, 473 pp., 1993.

Salvini R., Vanneschi C., Riccucci S., Francioni M., and Gullì D.: Application of an integrated geotechnical and topographic monitoring system in the Lorano marble quarry (Apuan Alps, Italy). Geomorphology, 241, 209-223, 2015.

Salvini, R., Mastrorocco, G., Seddaiu, M., Rossi, D., and Vanneschi, C.: The use of an unmanned aerial vehicle for fracture mapping within a marble quarry (Carrara, Italy): photogrammetry and discrete fracture network modeling, Geom .Nat. Haz. Risk, doi:10.1080/19475705.2016.1199053, 2016.

Formattato: Inglese (Regno Unito)

Formattato: Inglese (Regno Unito)

Shahbazi, M., Sohn, G., Théau, J., and Ménard, P.: UAV-based point cloud generation for open-pit mine modeling. Int. Arch. Photogramm. Remote Sens. Spat. Inf. Sci., 40, 313-320, 2015.

Spetsakis, M. E., and Aloimonos, J.: A multi-frame approach to visual motion perception. Int. J. Comput. Vision, 6, 245-255, 1991.

Stead, D., and Wolter, A.: A critical review of rock slope failure mechanisms: The importance of structural geology, J. Struct. Geol., 74, 1-23, 2015.

Stead, D., Eberhardt, E., and Coggan, J.S.: Developments in the characterization of complex rock slope deformation and failure using numerical modelling techniques, Eng. Geol., 83, 217-235, 2006.

Sturzenegger, M., and Stead, D.: The Palliser Rockslide, Canadian Rocky Mountains: Characterization and modeling of a stepped failure surface, Geomorphology, 138, 145-161, 2012.

Sturzenegger, M., and Stead, D.: Close-range terrestrial digital photogrammetry and terrestrial laser scanning for discontinuity characterization on rock cuts, Eng. Geol. 106, 163–182, 2009.

Tong X., Liu X., Chen P., Liu S., Luan K., Li L., Liu S., Liu X., Xie H., Jin Y., and Hong Z.: Integration of UAV-Based Photogrammetry and Terrestrial Laser Scanning for the Three-Dimensional Mapping and Monitoring of Open-Pit Mine Areas, Remote Sens., 7, 6635-6662, 2015.

Tuckey, Z., and Stead, D.: Improvements to field and remote sensing methods for mapping discontinuity persistence and intact rock bridges in rock slopes, Eng. Geol., 208, 136-153, 2016.

Vasuki, Y., Holden, E.J., Kovesi, P., and Micklethwaite, S.: Semi-automatic mapping of geological structures using UAV-based photogrammetric data: an image analysis approach, Comput. Geosci., 69, 22-32, 2014.

Vöge, M., Lato, M.J., and Diederichs, M.S.: Automated rockmass discontinuity mapping from 3-dimensional surface data, Eng. Geol., 164, 155-162, 2013.

Westoby, M. J., Brasington, J., Glasser, N. F., Hambrey, M. J., and Reynolds, J. M.: "Structurefrom-Motion" photogrammetry: A low-cost, effective tool for geoscience applications, Geomorphology, 179, doi:10.1016/j.geomorph.2012.08.021, 2012.

Zajc, M., Pogačnik, Z., and Gosar, A.: Ground penetrating radar and structural geological mapping investigation of karst and tectonic features in flyschoid rocks as geological hazard for exploitation, Int. J. Rock Mech. Min., 67, 78-87, 2014.

Zheng, D., Frost, J. D., Huang, R. Q., and Liu, F. Z.: Failure process andmodes of rockfall induced by underground mining: A case study of Kaiyang Phosphorite Mine rockfalls, Eng. Geol., 197, 145-147, 2015.

Table 1. Utilized RPAS and camera specifications.

RPAS Type	Dimensions (cm)	Engines	Rotor diameter (cm)	Empty weight (kg)	Max. takeoff weight (kg)
Aibotix Aibot X6 v1	Width 105 Height 45	Brushless motors	30.48 (12")	2.45	6.5
Camera	**Sensor type**	**Sensor Size (mm)**	**Image size (pixel)**	**Pixel size (mm)**	**Focal length (mm)**
Nikon CoolpixA	CMOS	23.6 x 15.6	4,928 x 3,264	0,0048	18.5

Table 2. Information related to the zenithal and frontal photogrammetric surveys and processing.

	ZENITHAL RPAS SURVEY	FRONTAL RPAS SURVEY
Number of images	151	448
GSD[1]	0.024 m/pixel	0.015 m/pixel
Relative flying altitude	93.9 m	60.7 m
# Tie Point	1,484,605	3,783,992
GCP[2] RMSE[3]	0.042 m	0.043 m
Check Point RMSE	0.065 m	0.03 m
GCP reprojection error	0.41 pixel	0.48 pixel

[1]Ground Sampleing Distance; [2]Ground Control Point; [3]Root Mean Square Error

Table 3. Characteristics of the discontinuity sets measured on the study area.

Set	Dip Dir/Dip (degrees)	Aperture (mm)	Filling	Persistence (m)	Spacing (m)	JCS (MPa)	JRC	Weathering	Water
K1	231/60	0-1	None, hard filling	2-10	0.1-0.3	50	2-6	Slightly weathered	Damp
K2a	234/86	0-0.5	Hard filling	5.5	5-10	60	2-4	Slightly weathered	Dry
K2b	66/86	0-0.5	Hard filling	5.5	5-10	60	2-4	Slightly weathered	Dry
K3a	142/81	0-2	None	<20	10-15	50	2-6	Slightly weathered	Damp
K3b	177/84	0-2	None	<20	10-15	50	2-6	Slightly weathered	Damp
K4	291/67	1-2	None	1-3	0.5-1.5	55	2-4	Slightly weathered	Damp

Tabella formattata

Table 4. Parameters used for RMRb determination. Chosen index values are underlined.

	Parameter	K1	K2a	K2b	K3a	K3b	K4
A1	Strength of intact rock material				7		
A2	RQD				(75%) 17		
A3	Spacing of discontinuities	15	20	20	20	20	15
A4	Condition of discontinuities	19	19	19	18	18	20
A5	Groundwater	10	15	15	10	10	10
	RMRb 67						

Table 45. Potentially unstable discontinuity systems along the two different slope orientations.

Slope	Planar sliding	Wedge sliding	Direct Toppling
50/90	K2b	K3a/K3b, K2b/K3a, K2b/K3b, K2b/K4, K2a/K4	K3a/K4, K1/K3a, K1/K4 (basal plane K2b)
323/90	K4	K1/K3b, K3b/K4, K1/K4, K2a/K4, K2b/K4	K3a/K3b, K2b/K3a, K2b/K3b, K1/K2b, K1/K2a, K2a/K2b (basal plane K4)

Table ~~5~~6. Characteristic of identified blocks A and B.

ID	Volume (m3)	Height (m)	Width (m)	Length (m)	Basal plane (Dip Dir/Dip)	Lateral release surface (Dip Dir/Dip)	Back discontinuity (Dip Dir/Dip)
A	2650	35	15	40	031/42	307/88	350/81
B	7500	40	20	32	031/35	307/88	-

Table 67. Results of the parametric analysis increasing basal plane cohesion values.

Rock bridge %	Intact rock (m^2)	Total cohesion (MN)	Driving force (MN)	Resisting force (MN)	Factor of safety
0	0	0	48.4	35.9	0.7
0.5	2.55	40.8	48.4	76.7	1.5
1	5.1	81.7	48.4	117.6	2.4
2	10.2	163.3	48.4	199.2	4.1
5	25.5	408.3	48.4	444.2	9.1
10	51	816.5	48.4	852.4	17.6

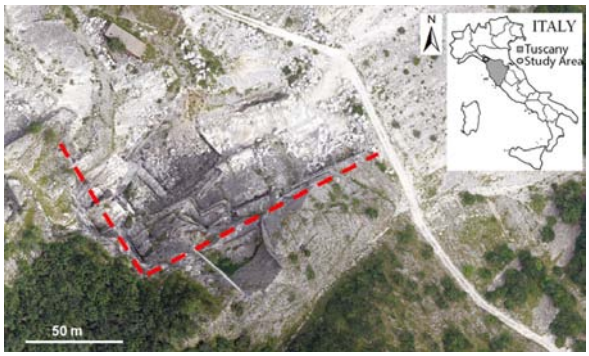

Figure 1. ~~Top~~ Plan view of the Piastrone open pit with indication of the two principal slope directions (dotted lines). Inset map shows the location of the study area.

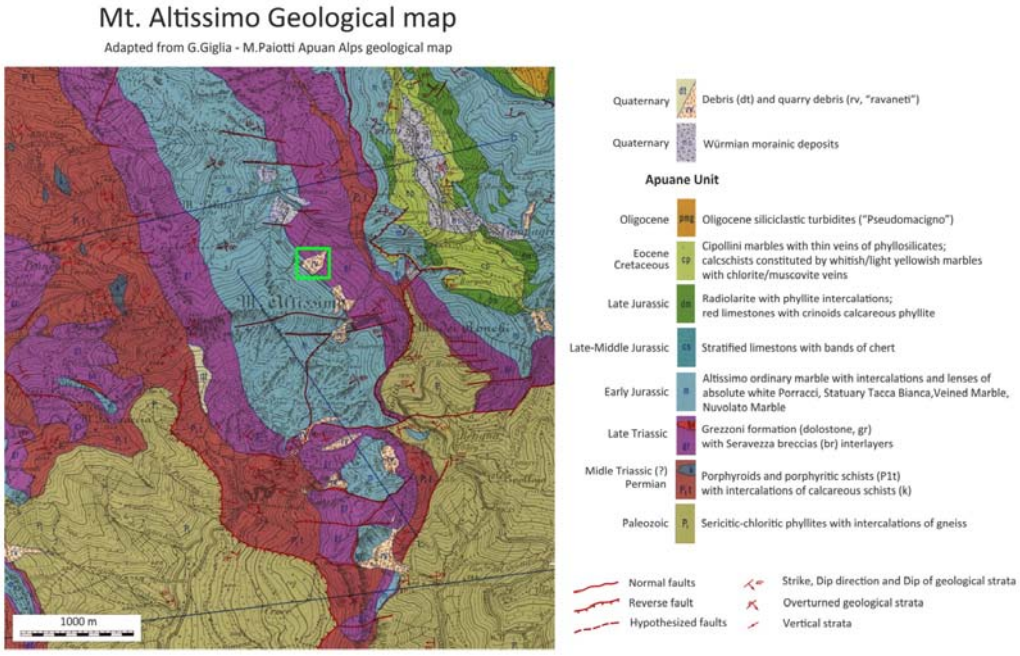

Figure 2. Geological map of the Mt. Altissimo area. The rectangle indicates the location of the quarry (modified from Giglia and Paiotti, 1963).

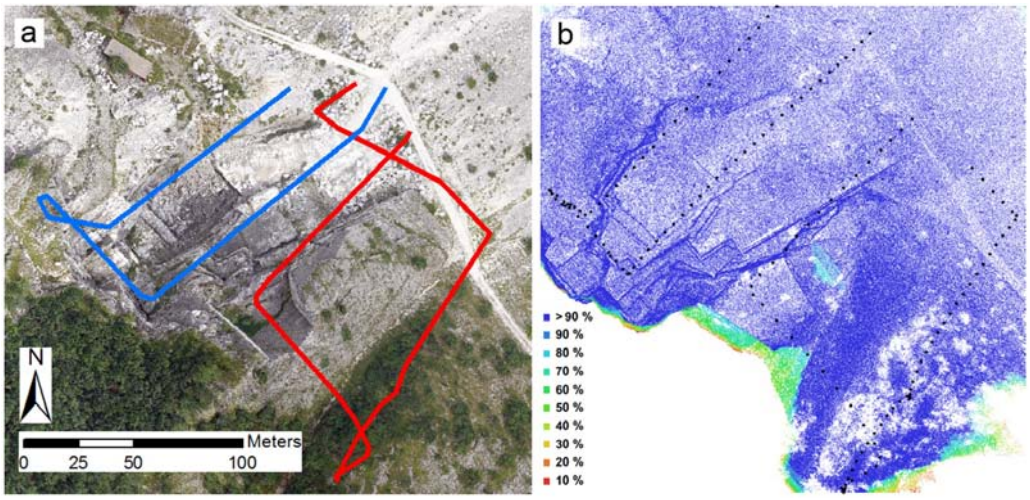

Figure 3. Flight paths of the RPAS zenithal surveys (a). ~~Top~~ Plan view of the area with indication of camera locations (black dots) and image overlap percentage (b).

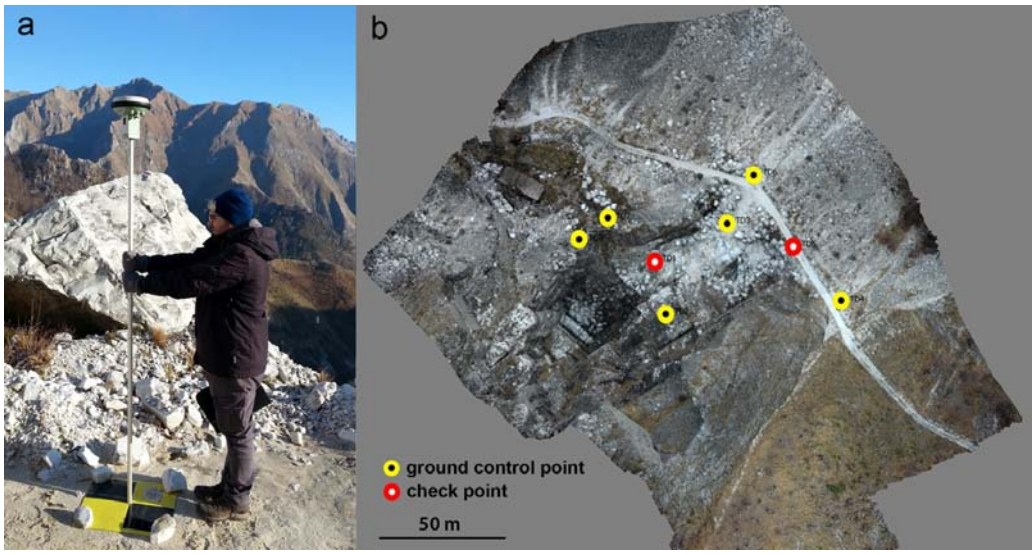

Figure 4. Example of a GCP measured during the RTK GNSS field survey (a) and spatial distribution of GCPs and check points for the RPAS zenithal flights (b).

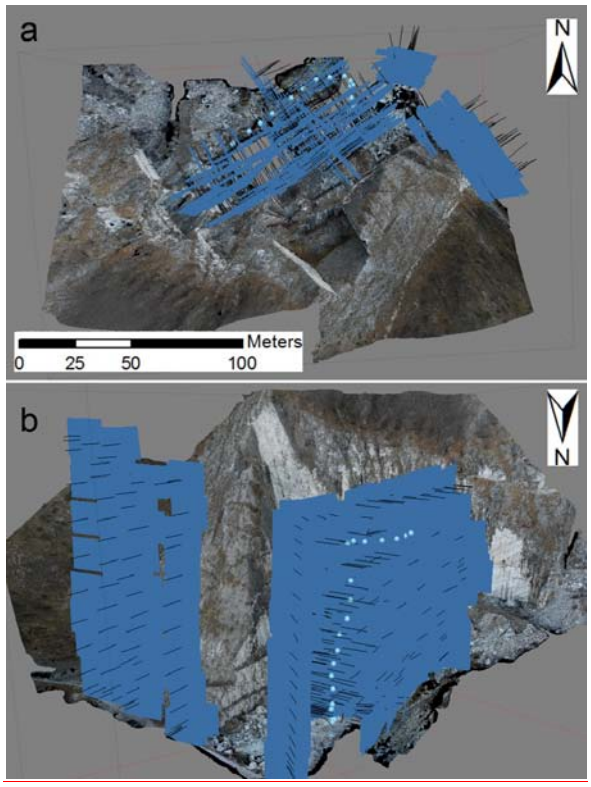
a
N
Meters
0 25 50 100
b
N

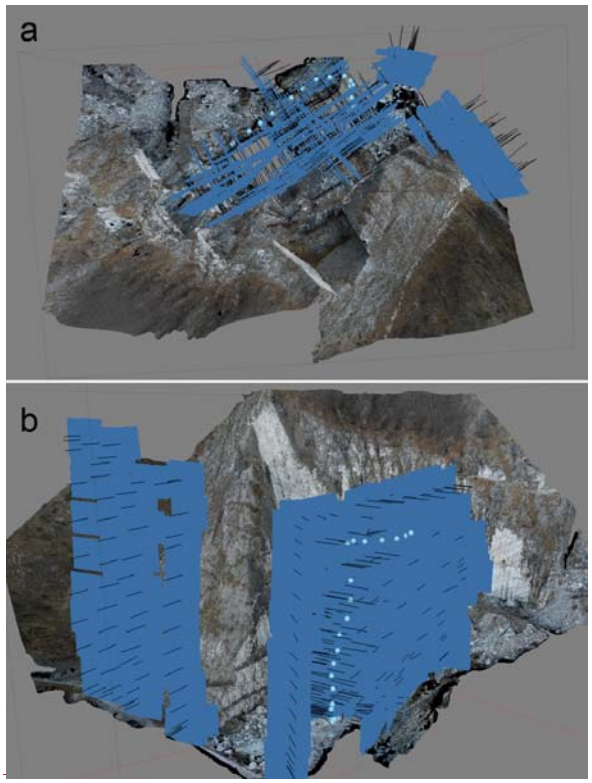

Figure 5. ~~Top~~ Plan view (a) and perspective view (b) of the RPAS frontal surveys (blue rectangles correspond to the photographs locations, black lines to normals). Corresponding 3D point cloud produced with photogrammetric processing of digital images is shown in background.

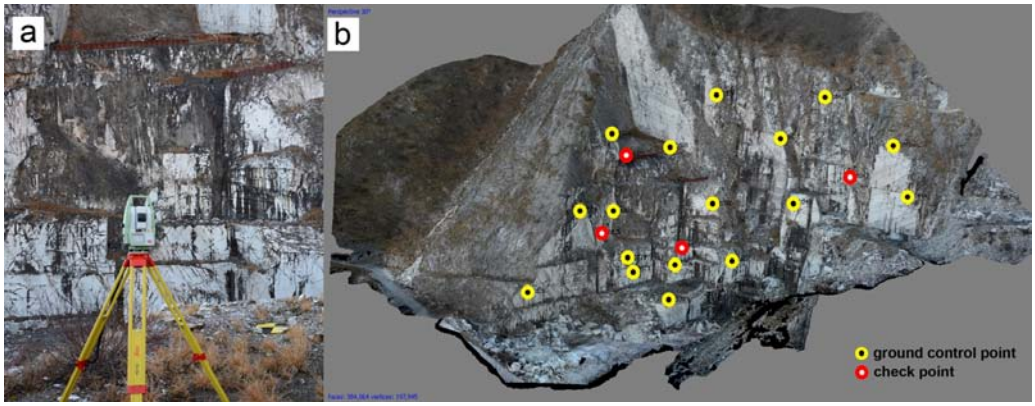

Figure 6. Topographic survey with TS (a) and spatial distribution of GCPs and check points for the RPAS frontal flights (b).

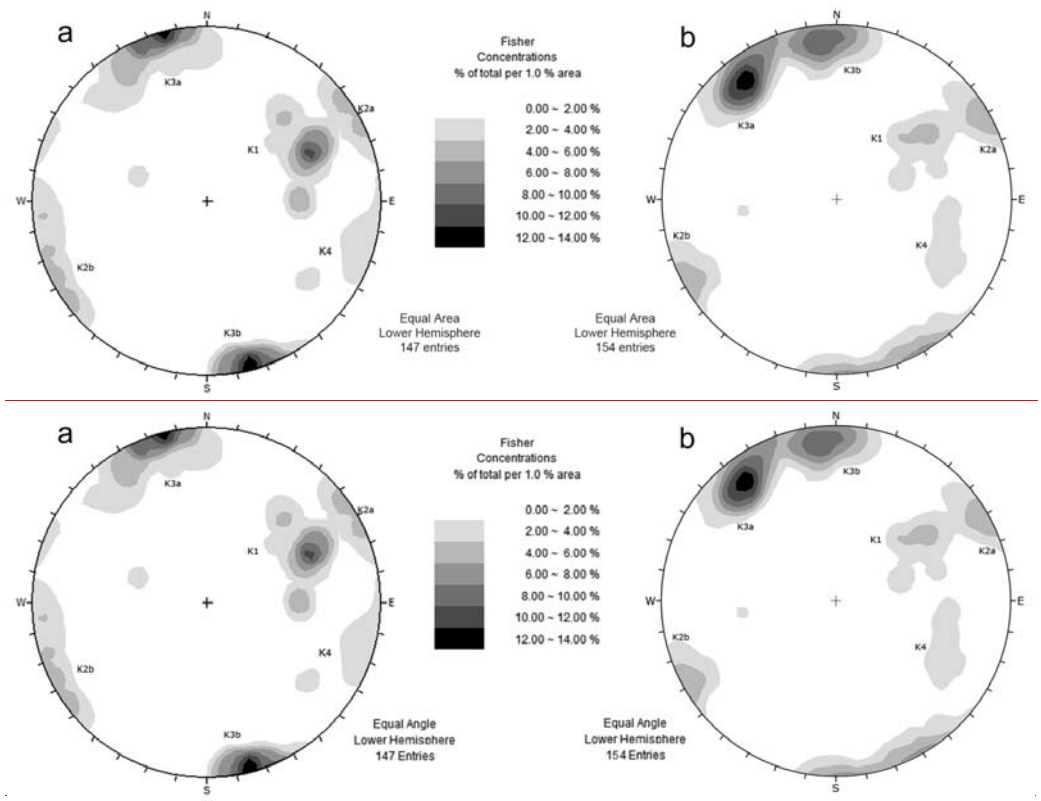

Figure 7. Stereonet plot of poles (Schmidt, equal area, lower hemisphere) of the discontinuities manually collected through classical engineering geological survey (a) and remotely collected by using photogrammetric data from RPAS surveys (b).

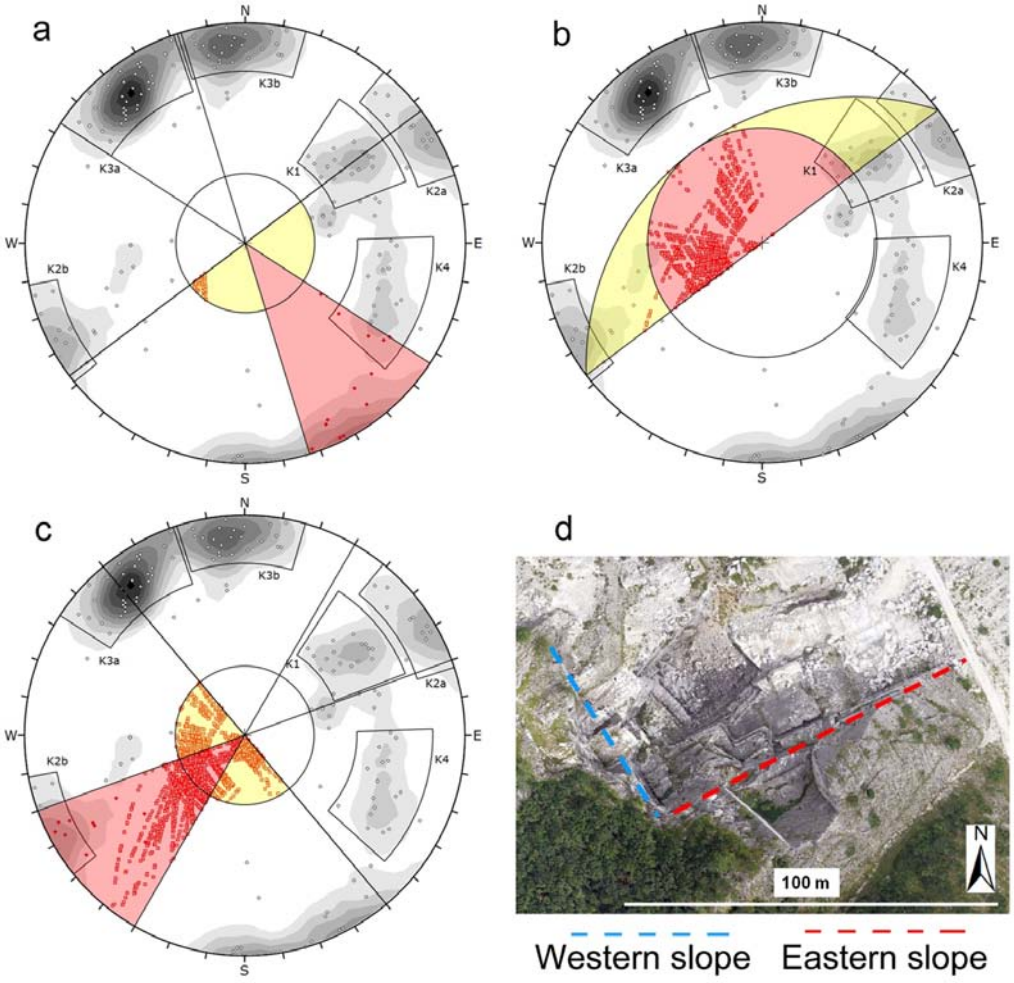

Figure 8. Examples of kinematic stability analysis carried out using Rocscience™ Dips 6.0 stereographic projection through the Wulff equal-angle method (lower hemisphere); a) Planar sliding on the eastern slope; b) Wedge sliding on the eastern slope; c) Direct toppling on the western slope; d) Aerial photo showing the two principal slope orientations.

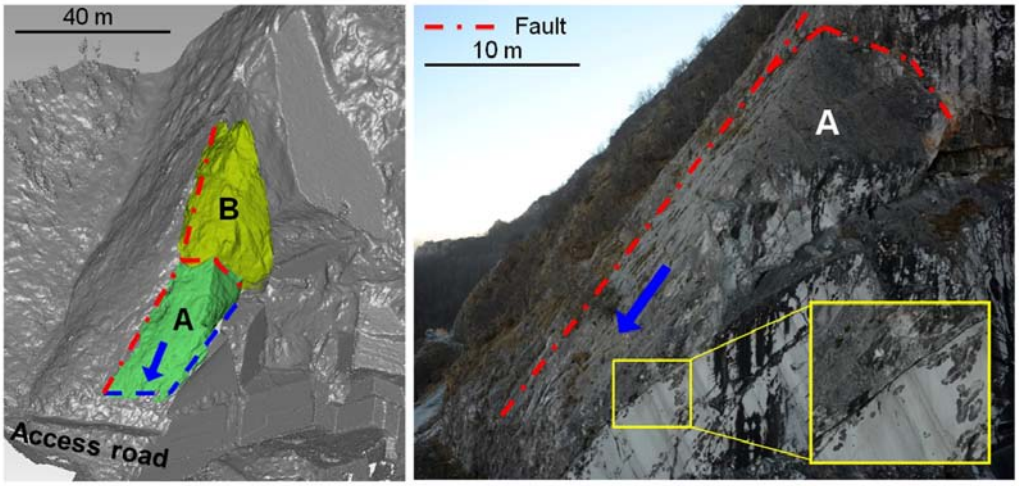

Figure 9. Identification of two large blocks with potential for sliding; inset photo highlights the visible aperture of the basal plane.

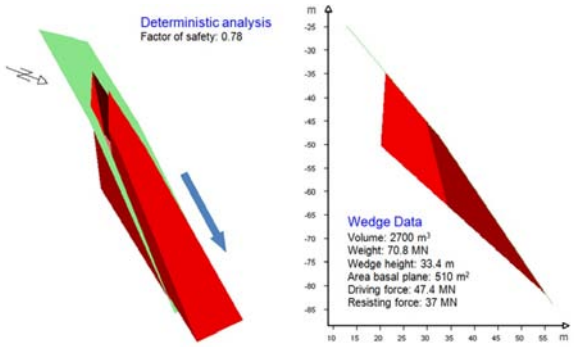

Figure 10. Result of Swedge 3D preliminary slope stability analysis.

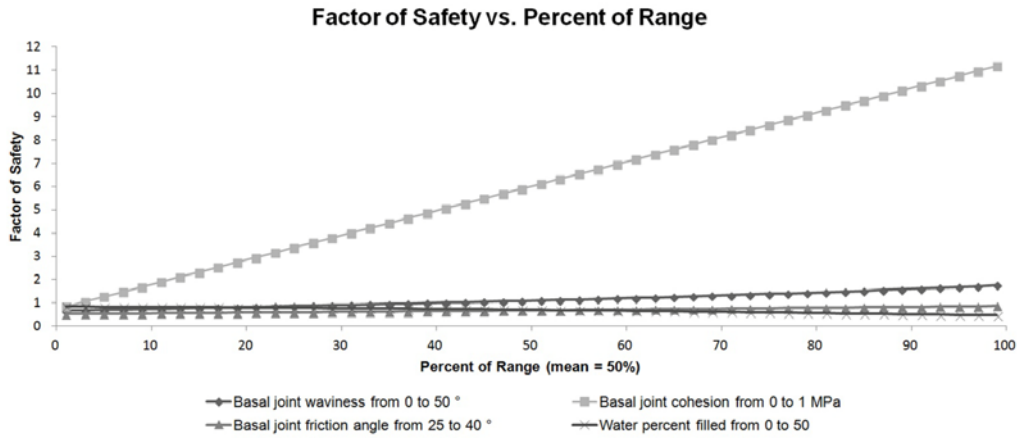

Figure 11. Result of sensitivity analysis relative to basal joint waviness, friction angle, cohesion and water percent filled parameters.

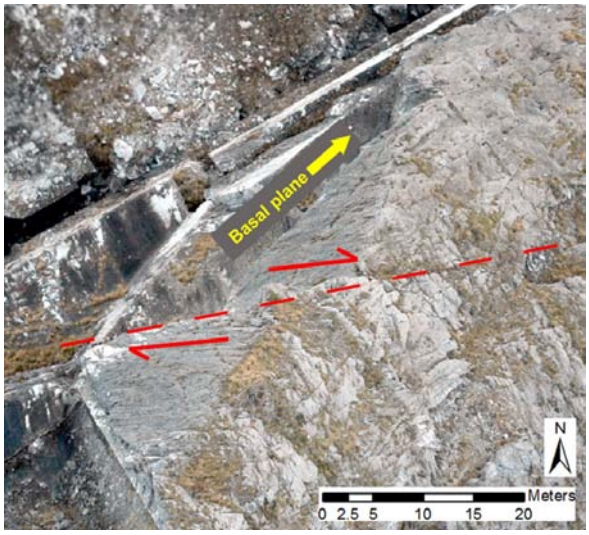

Figure 12. ~~Particular~~ Detail of the zenithal orthophoto with indication of apparent motion of a major fault acting as back release surface for block A of figure 9.

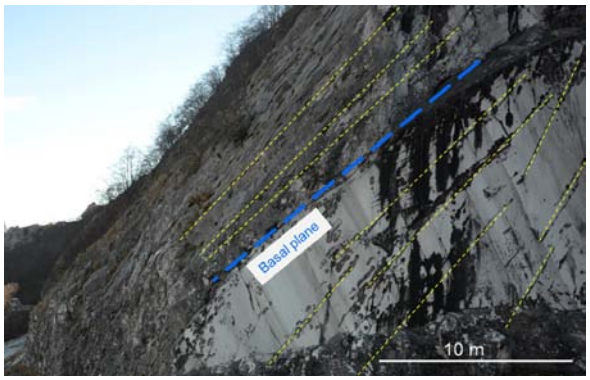

Figure 13. Details ~~Particular~~ of a series of thigh discontinuities over and below the basal plane under study.

Formattato: Tipo di carattere: Non Grassetto, Inglese (Stati Uniti)

Formattato: Tipo di carattere: Non Grassetto